Calibration and bore sighting of the topo-bathy lidar and RCD30 camera, 2015 mission

Prepared by

Tim Webster, PhD
Kevin McGuigan, Nathan Crowell, Kate Collins, Candace MacDonald, Sean Dzafovic, Matt Roscoe & David Kristiansen
Applied Geomatics Research Group, NSCC, Middleton
Tel. 902 825 5475
email: tim.webster@nscc.ca

Table of Contents

Table of Figures

List of Tables

1 Introduction

The 2015 surveys began on Oct. 22, 2015 and concluded Nov. 10, 2015. The surveys were conducted for 15 study sites throughout NS and NB. The calibration fights were conducted in Fredericton on Oct. 23, 2015 with ground truth RTK GPS checkpoints collect on Oct. 22 and 23, 2015.

2 Methods & Results

2.1 Calibration flight configuration

The flight lines for the calibration survey were planned over an area of urban building with variable relief and a mix of cleared, forested and urban areas in Fredericton, NB. The aircraft was owned and rented from leading Edge Geomatics for the surveys. Nathan Crowell operated the sensor during the calibration flights and for the remainder of the surveys. The flight lines were planned at flying heights of 1000 m and 400 m for topo only and topo-bathymetric surveys respectively (Figure 1). However due to poor weather conditions, only the 400 m above ground level (AGL) lines were flown and used. Since only topo-bathymetric surveys were conducted in 2015, this calibration set was all that was required. The calibration flights were carried out on Oct 23, 2015. Flight lines were flown in opposite directions for each line. Flight line overlap was planned at 30% for all lines and two sets of lines were flown in a perpendicular direction (Figure 1).

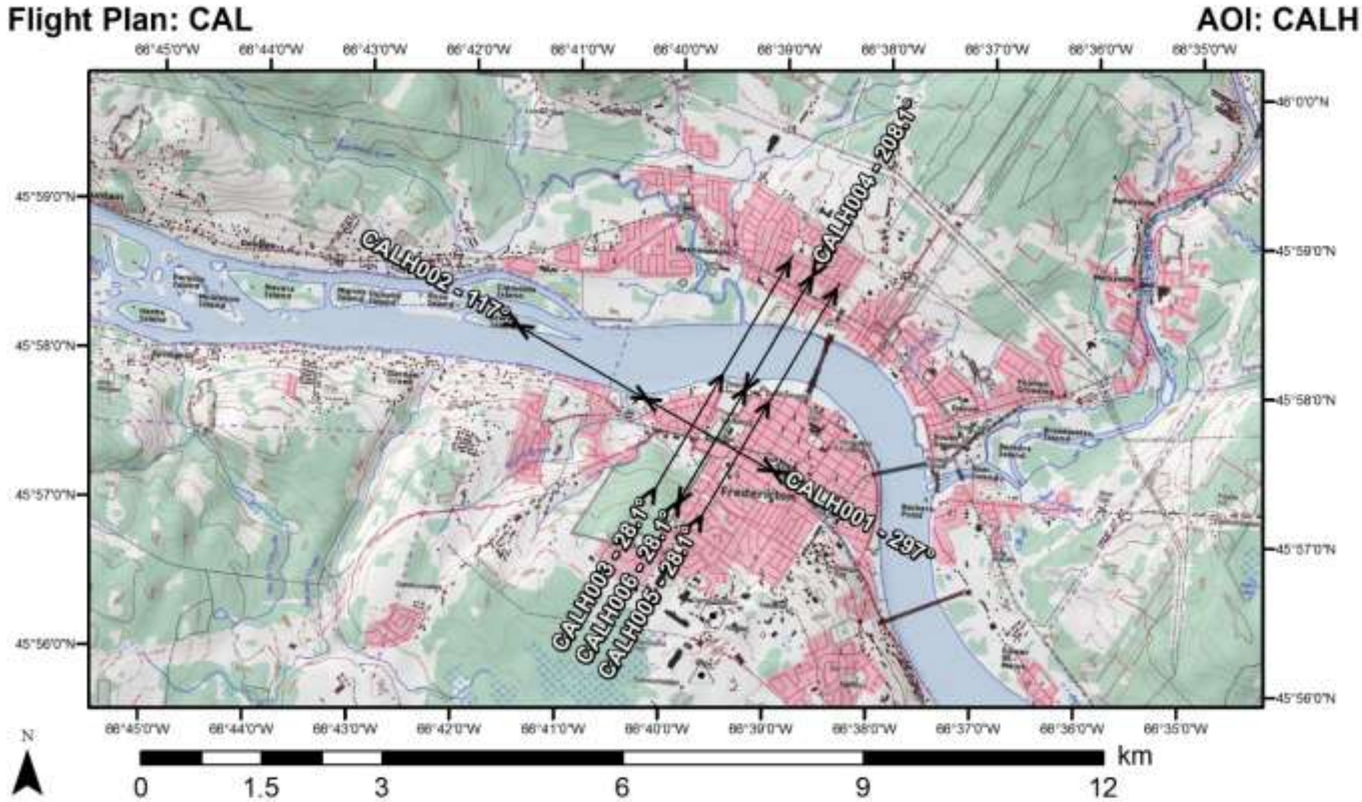

Figure 1 Planned flight lines for the lidar sensor calibration and RCD30 bore sighting.

2.2 Ground Survey Details

GPS surveys were conducted on Oct 22 and 23 to collect RTK checkpoints to be used in validating the absolute accuracy of the lidar and photo identifiable points to check the accuracy of the RCD30 orthophotos. The high precision network monument in Fredericton, Flemming Forest Ranger School was used as the base station for the ground control GPS surveys (Figure 2). The published coordinates for the HPN 941007 were obtained from Service NB and used in the setup (Figure 3). Two sets of GPS checkpoints were collected; one set were collected in for flat surfaces that could be used to validate the height of the lidar elevations, while the other points were collected at features that could be identified from the aerial photos collected with the RCD30. In many cases the photo identifiable points could also be used to validate the heights of the lidar elevations.

Figure 2 GPS base station used for RTK GPS surveys Oct. 22-23, 2015.

/onument	Name	Owner	DatePub	Status	DateInsp	Lat	Long	ElHt	E83CS	N83CS	OrthoHt
941007	:redericto	SNB	12/1/2013 0:00	LOC	9/28/2012 0:00	45° 56' 00.3921''	66° 39' 34.6067''	95.819	2487621.827	7437041.438	117.789

Figure 3 Coordinates of the HPN used as GPS base station for ground truth data.

An example of a common sets of GPS checkpoints for both the lidar elevations and the aerial photo positioning are the corners of the tennis courts (Figure 4). As can be seen in the photo of the tennis courts, Oct. 22 was an overcast day with periods of rain. Other checkpoints were collected in areas that represented the boundary between two features that were phot identifiable and had relief so that the horizontal position of the lidar surfaces could be examine (**Error! Reference source not found.**) such as the parking lot boundary at the Atlantic Superstore.

Figure 4 RTK GPS checkpoints collected along the edges of the tennis courts.

2.3 Laser calibration & Bore sighting RCD30

Once the flight lines have been flown and the aircraft trajectory processed (Figure 5). The GPS and IMU are combined to determine the best forward and backward trajectory (Figure 6) and the standard deviation of the position solution is also reported (Figure 7). The data are examined in Lidar Survey Studio where a calibration routine is applied to the data (Figure 8). Rough estimates were made of the lever arm offsets in the aircraft. These are the offsets between the inertial measurement unit (IMU) and the aircraft GPS antenna are refined using inertial explorer and are defined in (Table 1).

Table 1 Offsets between the GPS and the IMU.

Offset X direction (m)	Offset Y direction (m)	Offset Z direction (m)
-0.359	1.869	0.987

The internal offset and angular rotations between the IMU and lasers, both topo sensor 1 and hydro or sensor 2, are defined in the XML System Configuration file and should not change unless the Chiroptera II sensor has been disassembled. The system examines the overlapping flight lines and adjusts the data so there is minimum offset between sharp features such as roof tops and refines the lever arm offsets and angular rotations between the IMU, GPS and sensor (Figure 9).

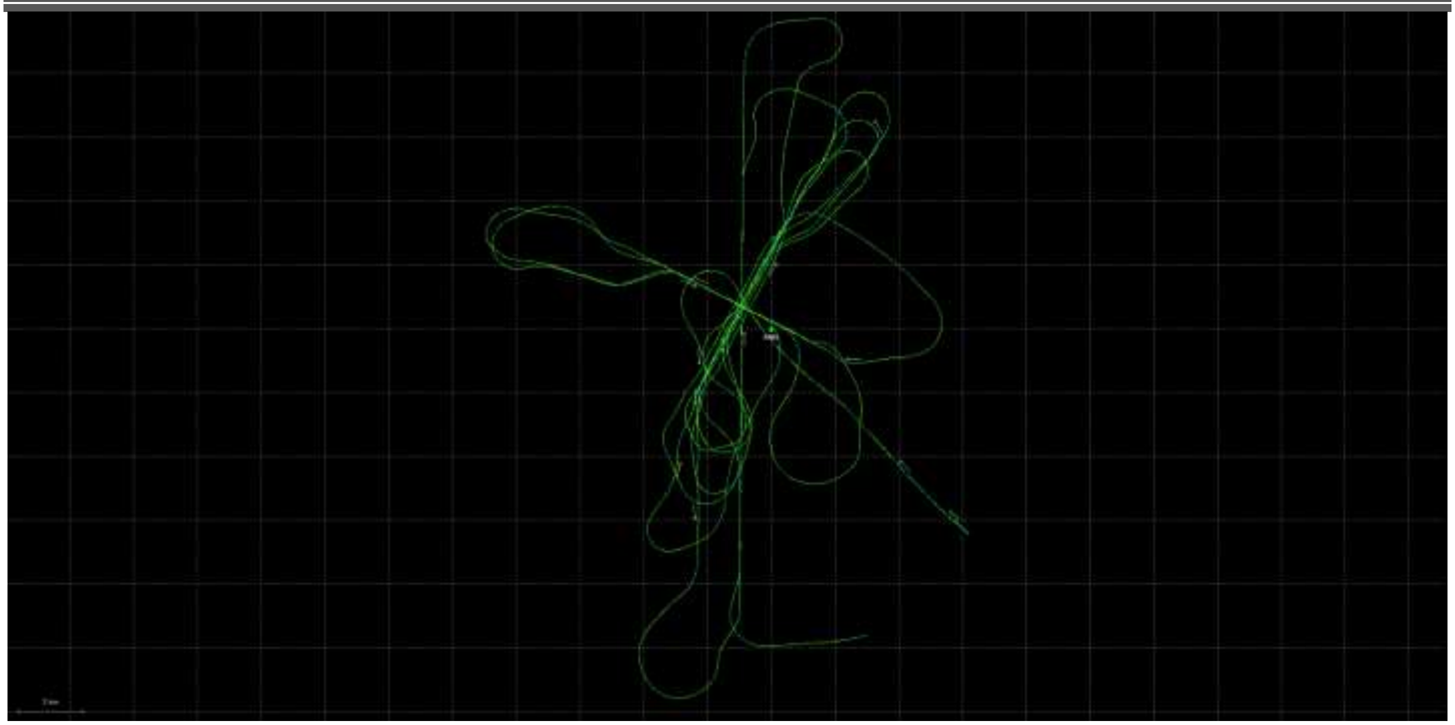

Figure 5 Trajectory of aircraft for flight lines used in the calibration process.

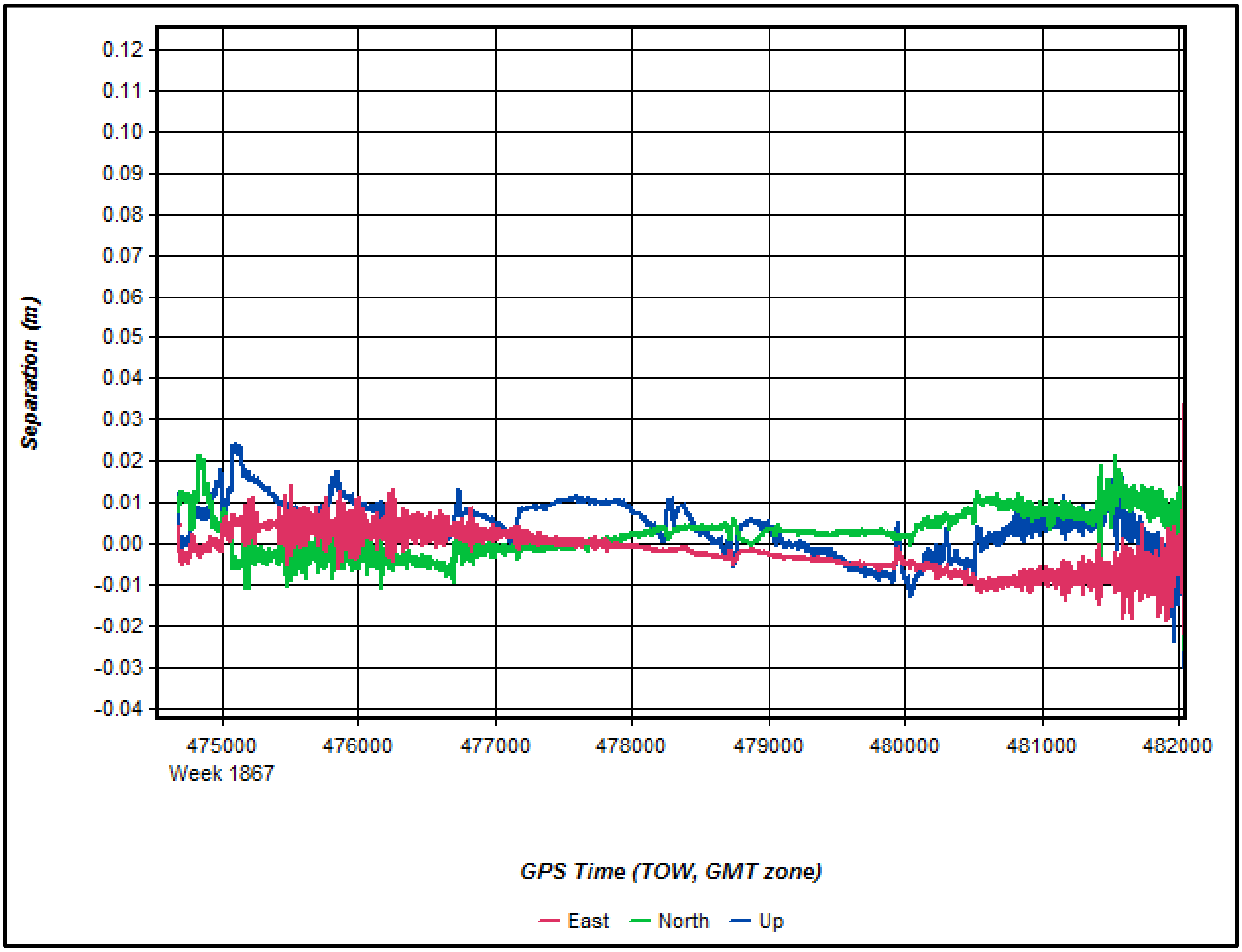

Figure 6 Estimate of positing errors of the trajectory.

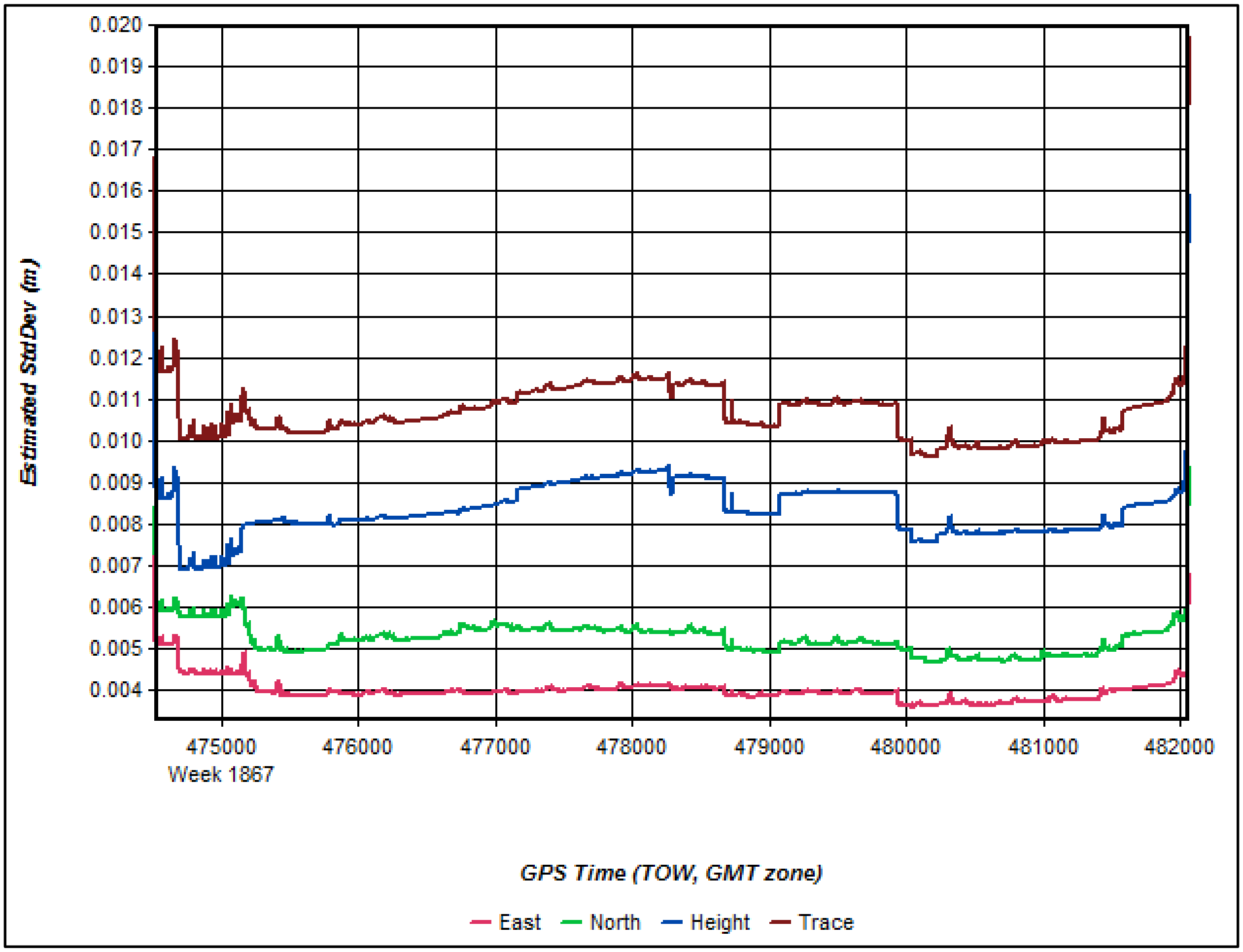

Figure 7 Standard deviation of the position solution of the aircraft.

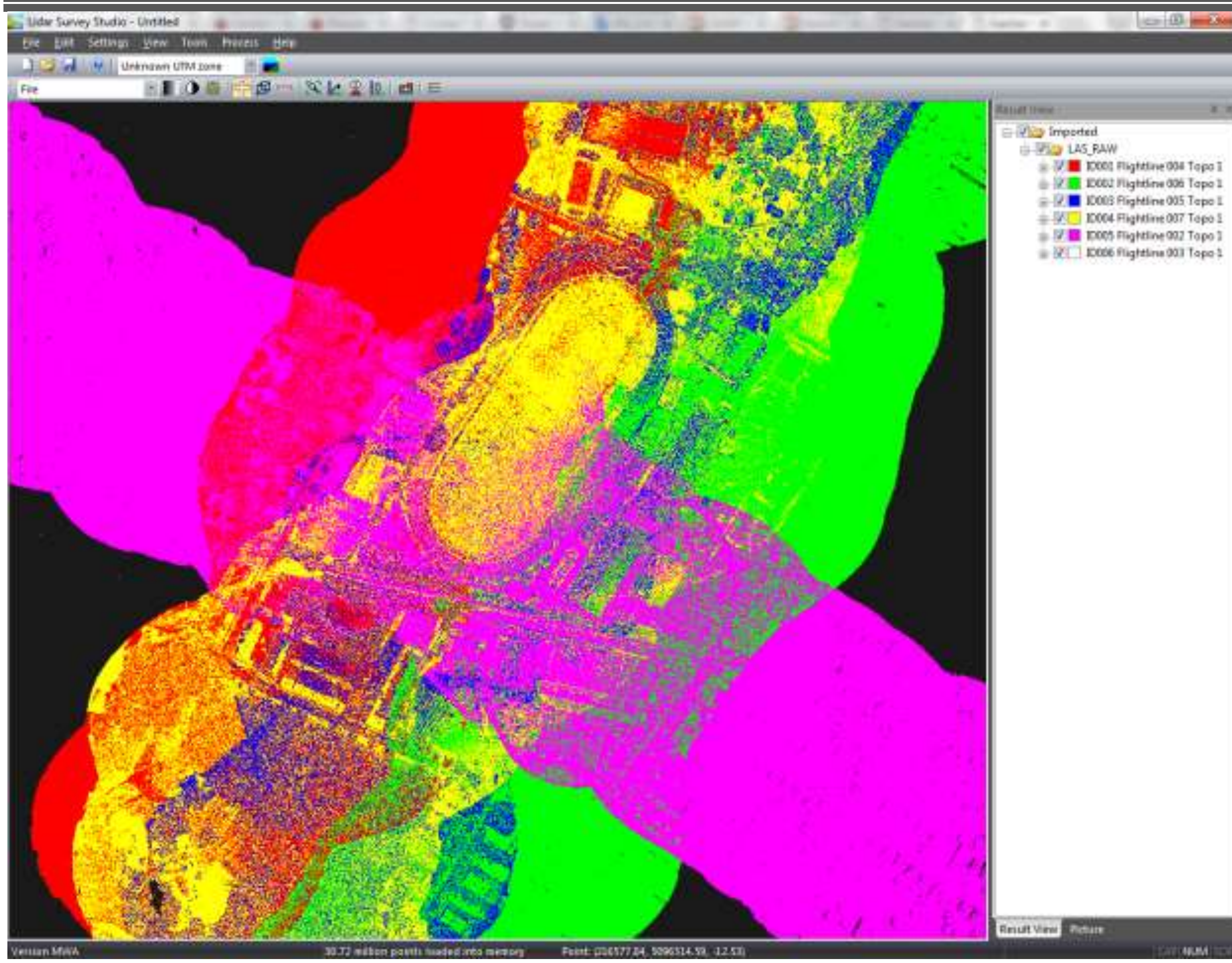

Figure 8 Flight lines over the calibration site showing topo laser return points.

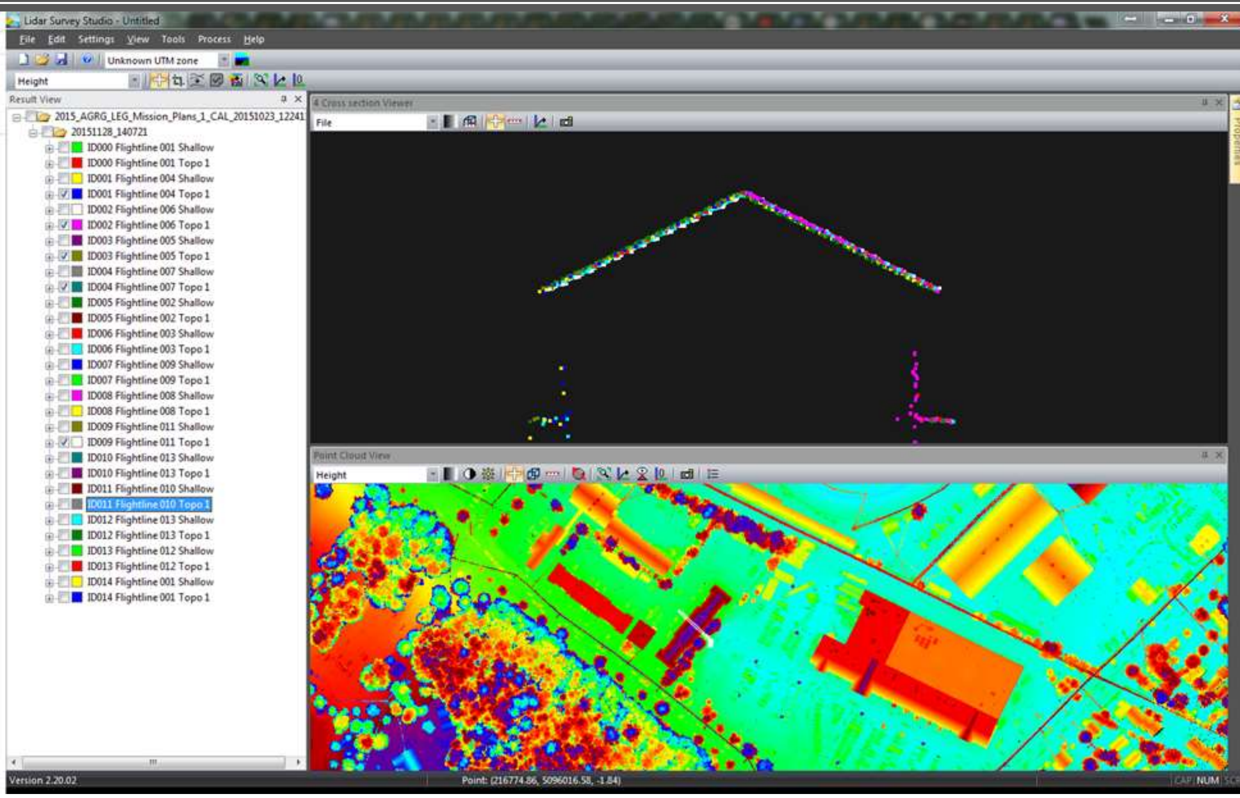

O

Figure 9 Overlapping flight line points (different colour per flight line) of a roof top in the calibration survey after the sensor has been calibrated.

The RCD30 camera frames over the calibration sight are used to “boresight” the camera to determine the lever arm offsets and angular rotations between the camera head and IMU using IPAS CO (Figure 10). The boresight parameters used for the survey wer3e determined and subsequently applied to the photo processing. These offsets and rotations are used in combination with the aircraft trajectory and timestamp to utilize direct georeferencing of the photos. Along with the direct georeferencing, the lidar bare-earth DEM was used to construct orthophotos which were then combined into a mosaic for each study area.

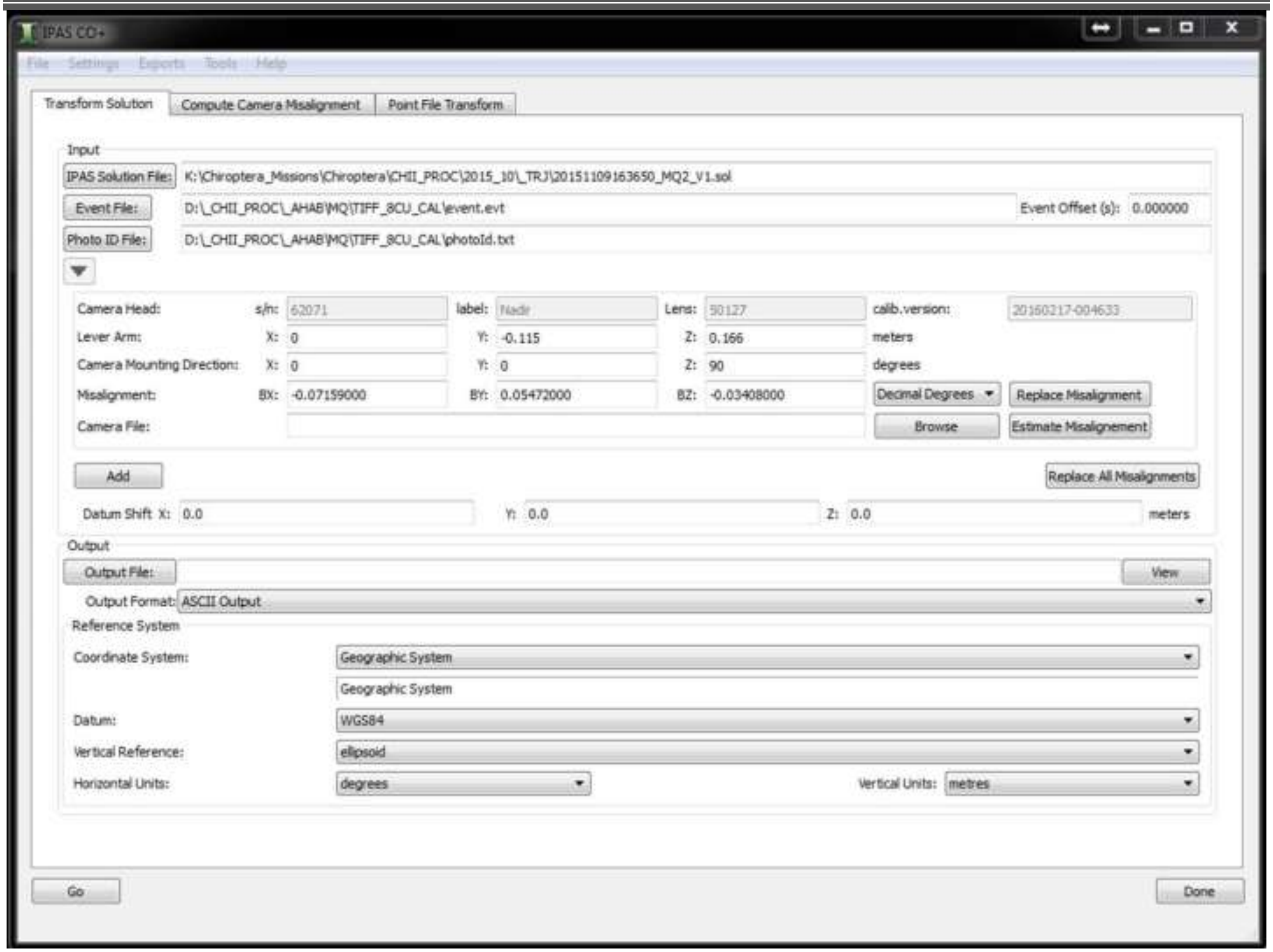

Figure 10 Boresight parameters for the RCD30 camera relating the camera head to the IMU.

Ground control GPS check points were compared against the 1 m raster DEM derived from the lidar. The lidar DEM in this case included the buildings (Figure 11). The total number of checkpoints used to validate the lidar data was 137. The difference between the measured GPS elevation was compared to the lidar DEM elevation and the difference in elevation calculated. The difference in elevation between the GPS and DEM distribution had a mean = -0.08 m, and a standard deviation = 0.03 m, with a RMSE = 0.09 m. The difference in elevation appears to be normally distributed indicating no bias with the exception that the DEM is approximately 8 cm too high (Figure 12).

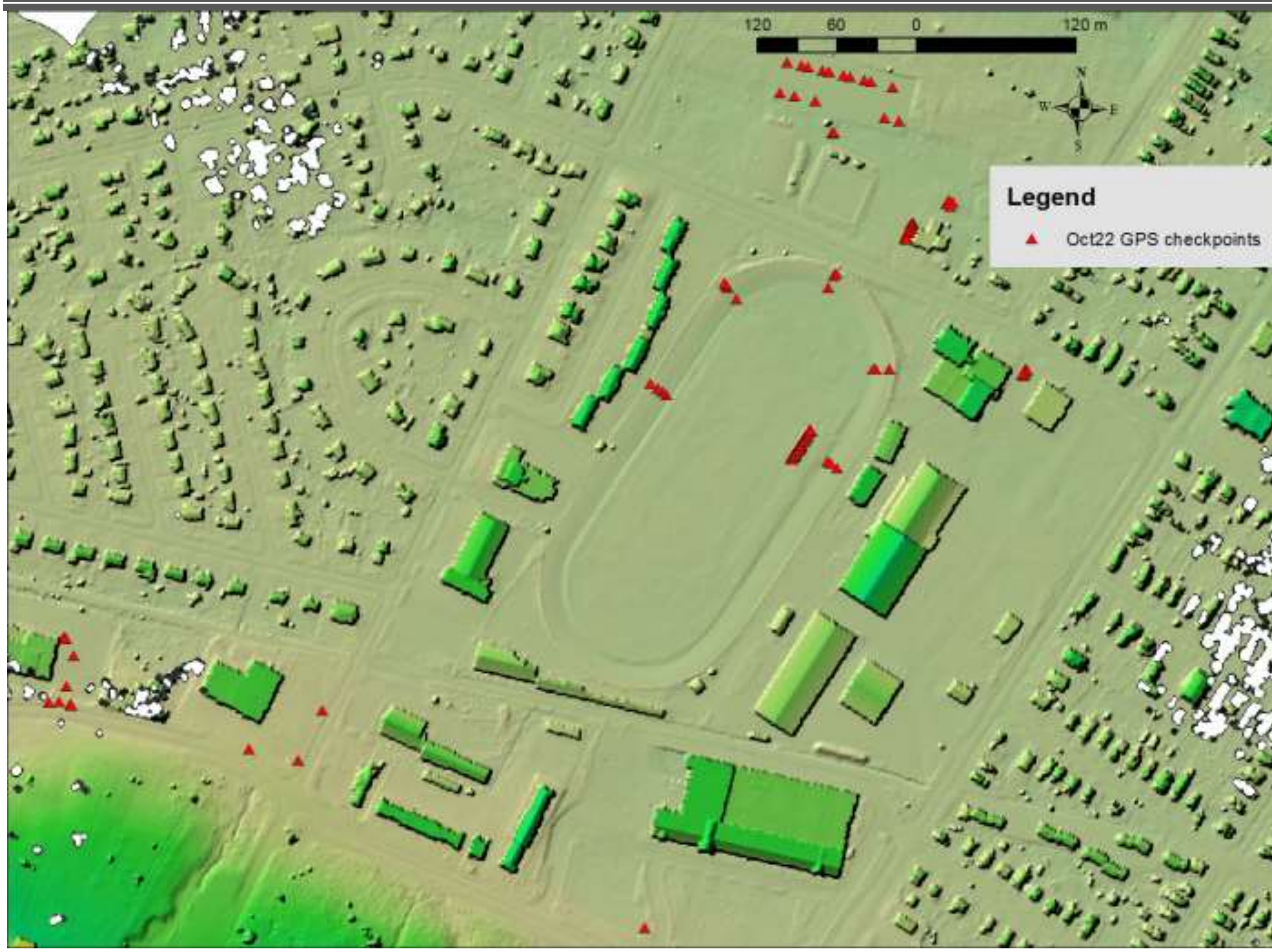

Figure 11 Lidar derived DEM of downtown Fredericton (horse racetrack visible) with GPS checkpoints (red triangles).

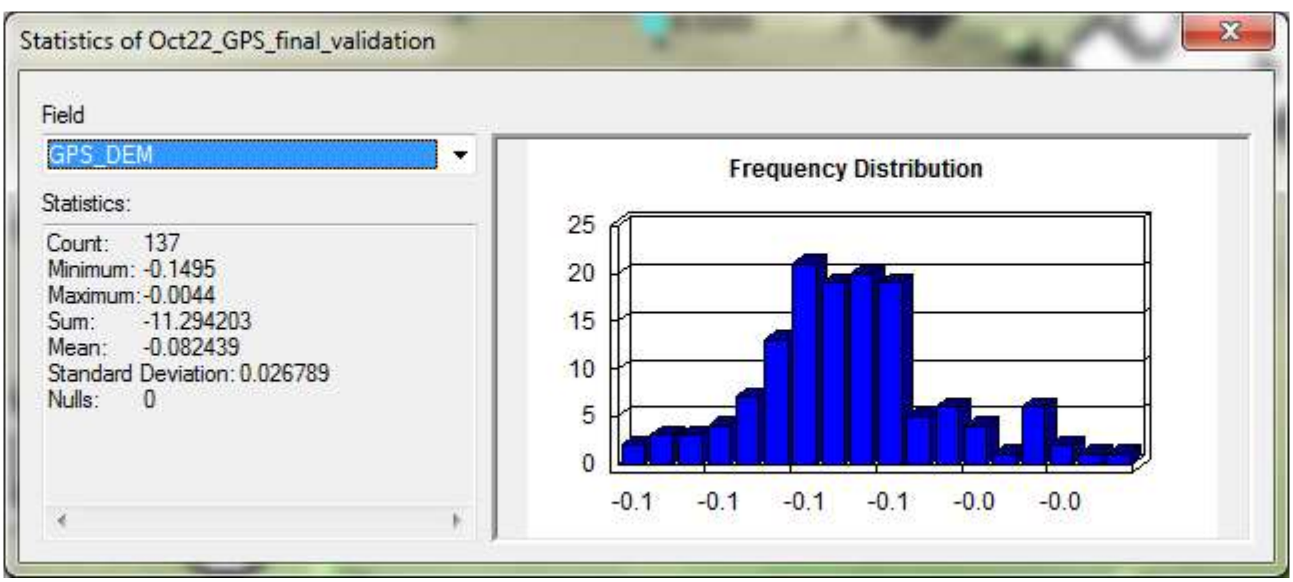

Figure 12: Distribution of the elevation difference (GPS-DEM) for the GPS checkpoints in Fig. 11.

The results from the camera calibration were evaluated by comparing photo identifiable GPS with the RCD30 imagery. In this case GPS points were collected at the edges of features that could be distinguished in the orthophoto (Figure 13). The edges of the tennis courts were collected as seen in Figure 4.

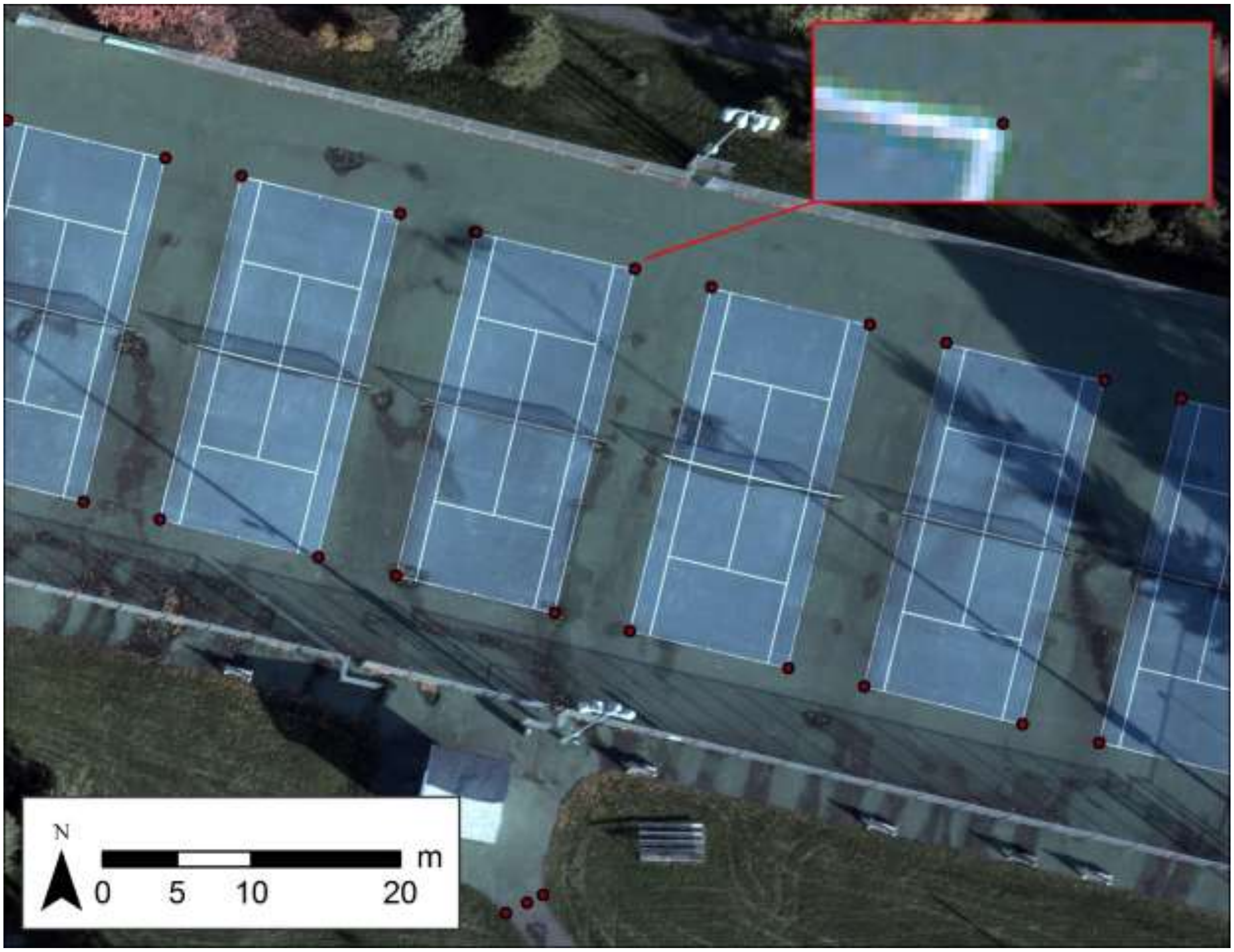

Figure 13 Example of GPS checkpoints compared to the orthophoto mosaic of the tennis courts in Fredericton.

3 Conclusions

The validation of the data which was used in the calibration process resulted in lidar and orthophoto map products to be produced that were within the specification of the system. The lidar elevations were within the specifications of 15 cm and the RCD30 photos were processed to 5 cm orthophotos with a horizontal positional accuracy of 1-2 pixels